frontiers | Frontiers in Earth Science

TYPE Original Research
PUBLISHED 06 January 2023
DOI 10.3389/feart.2022.1015832

OPEN ACCESS

EDITED BY
Hu Li,
Southwest Petroleum University, China

REVIEWED BY
Jianguo Zhang,
China University of Geosciences, China
Liuqin Chen,
East China University of Technology, China
Li Hongbo,
Yangtze University, China

*CORRESPONDENCE
Xingchao Jiang,
22195067@qq.com
Long Huang,
116643724@qq.com

SPECIALTY SECTION
This article was submitted to Structural Geology and Tectonics, a section of the journal Frontiers in Earth Science

RECEIVED 10 August 2022
ACCEPTED 20 September 2022
PUBLISHED 06 January 2023

CITATION
Wang M, Jiang X, Lei B, Huang L and Pan J (2023), Tectonic evolution and its control on oil–gas accumulation in southern East China Sea since the Jurassic.
Front. Earth Sci. 10:1015832.
doi: 10.3389/feart.2022.1015832

Tectonic evolution and its control on oil–gas accumulation in southern East China Sea since the Jurassic

Mingjian Wang[1,2], Xingchao Jiang[3,4]*, Baohua Lei[1], Long Huang[1]* and Jun Pan[1]

[1]Qingdao Institute of Marine Geology, China Geological Survey, Ministry of Natural Resources, Qingdao, China, [2]Laboratory for Marine Mineral Resources, Pilot National Laboratory for Marine Science and Technology, Qingdao, China, [3]Hubei Key Laboratory of Petroleum Geochemistry and Environment, Yangtze University, Wuhan, China, [4]Key Laboratory of Exploration Technologies for Oil and Gas Resources, Ministry of Education, Yangtze University, Wuhan, China

Based on the results from the previous research on Mesozoic igneous rocks, as well as tectonic environments in the northern South China Sea and southern East China Sea (NSCS-SECS), geophysical parameters, strata, and characteristics of seismic facies in NSCS-SECS were investigated. These findings were combined with results from the analysis of the balanced profile evolution to re-evaluate the tectonic evolution of SECS since the Jurassic. Furthermore, burial history and simulation of wells in the SECS were analyzed using well, seismic and source rock data. Furthermore, favorable models of oil–gas accumulation in the Lower–Middle Jurassic were proposed in combination with studies on elements and conditions of the petroleum system. The results demonstrated that the NSCS-SECS had consistent tectonic settings and comparable strata from the Jurassic to the Cretaceous time. There was a large unified basin in this period. The basin experienced two evolutionary stages, respectively, the fore-arc depression basin in the Early–Middle Jurassic ($J_{1\text{-}2}$) and the back-arc faulted basin in the Late Jurassic–Cretaceous (J_3-K). There was considerable deposition of dark mudstones in the SECS during the Lower–Middle Jurassic. The Keelung Sag was the depositional center accumulating the thickest section of the Lower–Middle Jurassic source rocks which entered a high-maturity stage. Hence, it was the hydrocarbon generation center in the SECS. The process of generating hydrocarbons from Lower–Middle Jurassic source rocks was of high complexity from northwest to southeast. The Lower–Middle Jurassic source rock at the northwest edges of the basin experienced two hydrocarbon generation stages, while the Keelung Sag toward the southeast experienced three hydrocarbon generation stages. The models and types of oil–gas accumulation in various evolutionary phases were different due to the control by tectonic evolution. Oil and gas that were generated by Lower–Middle Jurassic source rocks in the Keelung Sag migrated and accumulated in the western high-tectonic units. Research findings provide insights into Mesozoic oil and gas exploration in the NSCS-SECS.

KEYWORDS

Early–Middle Jurassic, tectonic evolution, source rocks, burial history, accumulation models, southern East China Sea

1 Introduction

The East China Sea Basin is a large overlapping Mesozoic–Cenozoic petroliferous basin in offshore China. It has experienced multiple stages of tectonic deformation since the Mesozoic and has complex geological conditions (Zheng et al., 2005; Yang et al., 2012, 2019; Zhong et al., 2018; Wang et al., 2020). Oil and gas exploration in the East China Sea Basin is divided into two stages, before and after 2005: 1) exploration was primarily focused on Cenozoic reservoirs prior to 2005; 2) Mesozoic reservoirs were better understood due to improvement in seismic acquisition and processing technology after 2005. Thus, oil and gas exploration gradually moved to deep strata. However, some challenges were experienced: 1) the study area was located in the junctional zone between the Eurasian Plate, Pacific Plate, and India–Australia Plate from the Mesozoic to Cenozoic time and experienced high-complexity evolution of the Yanshan Movement, as well as a strong reconstruction of the Himalayan Movement, resulting in complex tectonic characteristics; 2) there were relatively limited drilling core and geophysical data in the study area.

Previous studies have mainly discussed the offshore geological conditions from adjacent onshore areas. Tectonics, geochemistry, and ancient geography remain controversial in the Mesozoic tectonic structures of SECS (Zheng et al., 2005; Yang et al., 2012, 2019; Suo et al., 2015; Chen et al., 2016; Xu et al., 2016, 2017; Li et al., 2017; Zhong et al., 2018; Zhang et al., 2019; Si et al., 2021).

Li et al. (2012) indicated for the first time that the NSCS-SECS may be a large unified sedimentary basin during the Mesozoic, and this was based on seismic and well data combined with gravity and magnetic inversion results in the SECS. He postulated that the western boundary of the Jurassic Basin was the Yandang old uplift. There were continuous extensive distributions of Mesozoic strata in the NSCS-SECS and the sedimentary depth gradually decreased from southwest to northwest (Qiu and Wen, 2004; Li et al., 2014). Xu et al. (2017) discovered an early Cretaceous igneous belt with a NE trend in the NSCS-SECS. Zhou (2002) identified a NE trend Mesozoic subduction accretion zone in NSCS, which was likely to be extended toward the SECS. Both the igneous belt and the subduction accretion zone were related to the movements of the old Pacific Plate (Zhou et al., 2005; Xu et al., 2017), suggesting that the NSCS-SECS was under the influence of the same setting tectonic during the Mesozoic. The analysis of gravity and magnetic inversion and well data suggests that the Mesozoic basement underlying the sedimentary rocks in the NSCS-SECS was the extension of the Caledonian Fold Belt in Southern China toward offshore areas (Lu et al., 2011; Sun et al., 2014), showing consistent basement properties. Overall, the NSCS-SECS showed similar and comparable features in terms of Mesozoic igneous lithology, geochemical signatures, tectonic environment, formation age, geophysical properties, and sedimentary strata.

In the SECS, previous studies have mainly focused on the Cenozoic basin structure, evolution, as well as Cenozoic oil and gas resource potential, which have achieved considerable results (Zheng et al., 2005; Sun et al., 2017; Zhong et al., 2018). However, there were relatively fewer studies on the Mesozoic geological structures. Currently, the evolutionary process of the Mesozoic Basin, including the basin type, the dynamic mechanism, as well as the generation and accumulation of hydrocarbons based on Mesozoic source rocks are still under debate (Yang et al., 2012; Yang et al., 2017; Yang et al., 2019; Wang et al., 2019; Wang et al., 2020; Wang et al., 2022a; Xiao et al., 2019; Liu et al., 2020). These limited understandings of Mesozoic tectonic evolution and oil and gas resource potentials.

From the comparative analysis of the Mesozoic basin basement, sedimentary strata, and dating of magmatic rocks combined with the analysis of regional tectonic dynamics in the NSCS-SECS, it is believed that the NSCS-SECS was a large unified basin in the Mesozoic period. These findings guided our discussion throughout these periods. Based on this, Jurassic oil and gas accumulation elements and conditions in the SECS were systematically analyzed, and favorable accumulation models were proposed to provide a geological basis for oil and gas exploration.

2 Geological setting

Mesozoic is the most important tectonic revolutionary period in eastern China. During this period, the evolution from the Indosinian tectonic domain to the Coastal Pacific tectonic domain was completed, and the complex tectonic settings and evolutionary process in offshore eastern China were formed. The NSCS-SECS area covered the present-day East China Sea Basin, the West Taiwan Basin, the southwest Taiwan Basin, and the east-central region of the Pearl River Mouth Basin (eastern side of the Yangjiang–Yitong'ansha Fault). It extended to the northern Yandang Swell in the East China Sea Shelf Basin as the northern boundary, the Yangjiang–Yitong'ansha Fault as the southwest boundary, and the Bijia Uplift–Diaoyu Island Fold Belt as the southeast boundary. It was separated from the mainland in the northwest by the Changle–Nan'ao Fault (Figure 1). The NSCS-SECS was generally NE-NNE trended. It was mainly controlled by NEE-NE-NNE trend faults from south to north, followed by the NW trend fault. The study area was chosen as the southern region of the East China Sea, located in the northern

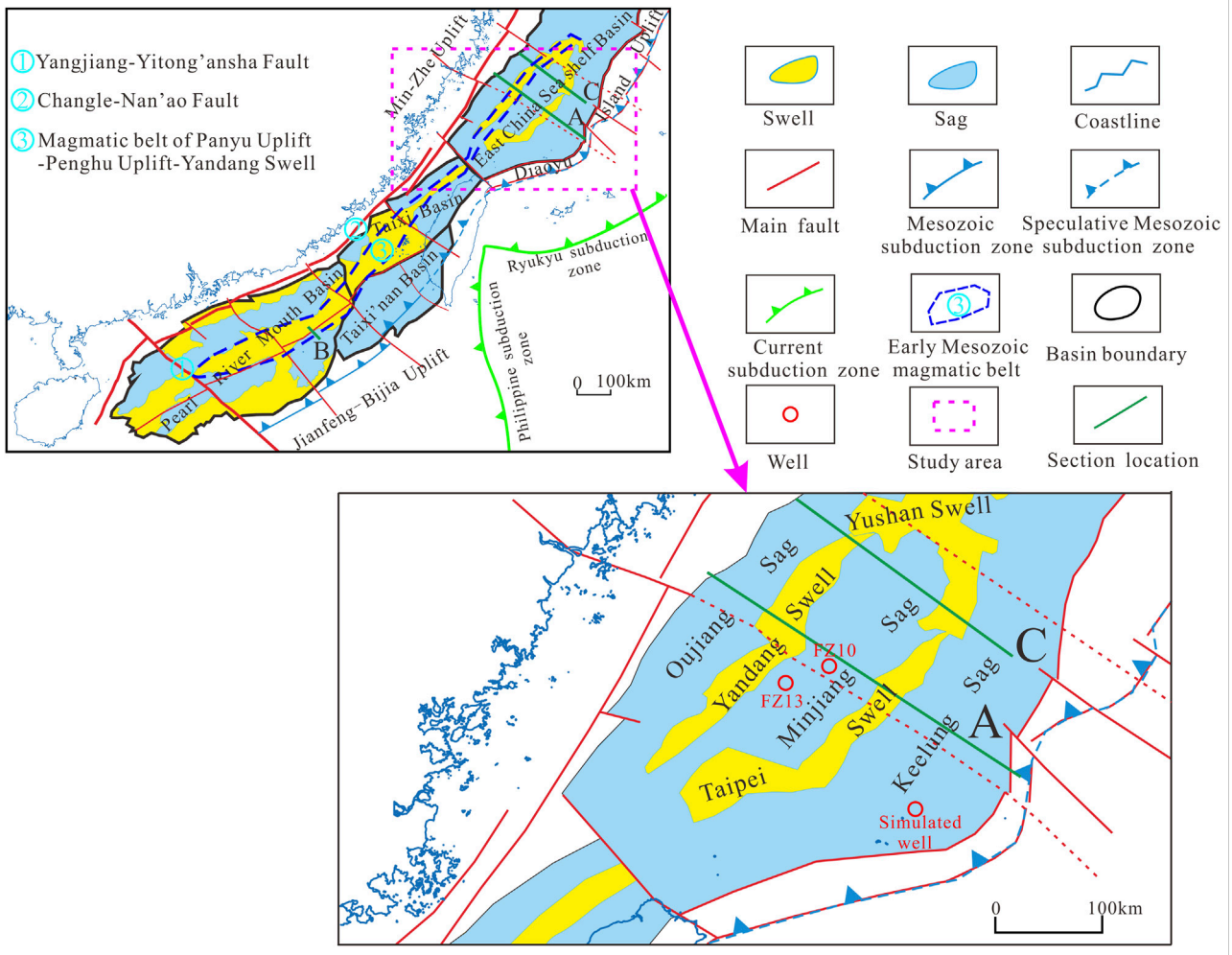

FIGURE 1
Overview of tectonic configurations along the NSCS-SECS. The current tectonic map of the SECS Basin is shown at the bottom right (modified from Zhou et al., 2005; Lu et al., 2011; Sun et al., 2014; Li S. et al., 2018).

region of the NSCS-SECS area. The study area was bounded by the Diaoyu Island Fold Belt to the east, West Taiwan Basin to the south, Zhemin Uplift Zone to the west, and separated from the northern region of the basin by the Yushan Swell to the north (Figure 1).

Rocks underlying the basin are similar to the Caledonian–Early Indosinian metamorphic rocks in South China, showing lithological consistency with onshore areas in Zhejiang and Fujian provinces (Yang et al., 2019). Sedimentary processes forming strata were dominant since the Mesozoic, among which the Jurassic–Cretaceous systems were mainly marine and paralic facies (Yang et al., 2015). The Cenozoic Basin covered a large area and the sedimentary environment was generally characterized by marine facies in the south and continental facies in the north (Zhong et al., 2018). Although controlled by NE-NNE trend faults, the East China Sea Basin has a characteristic tectonic distribution of NE trend belts intersected by NW faults. There were five tectonic units in the basin from west to east, namely, Oujiang Sag, Yandang Swell, Minjiang Sag, Taibei Swell, and Keelung Sag. Jurassic strata were developed in the tectonic units east of the Oujiang Sag.

3 Data and methods

The main data used in this article, including strata thickness data, lithological data, vitrinite reflectance (R_o) from dark mudstone and coal seams, and sandstone reservoir properties, were collected by oil and gas resource strategic research projects and published articles over the past 10 years. Additional

information from gravity and magnetic results published by Zhang et al. (2010) was also included in the data package. The study benefited from seismic reflection data provided by the Qingdao Institute of Marine Geology, Geological Survey of China.

The region from NSCS to SECS was considered in this study as one entity and was placed in the unified Mesozoic geotectonic settings. The basin evolution and the dynamic mechanism focusing on regional dynamic analysis since the Jurassic were discussed combining analysis of the typical balanced seismic profile from the SECS. The kerogen type and vitrinite reflectance (R_o) were measured by the fluorescence microscope and optical microscope. Reservoir porosities were obtained from the core test, observation of thin section in the core sample, and interpretation of logging data. Lower–Middle Jurassic source rock quality, reservoir properties, and seal rock development were systematically analyzed based on seismic and well data (FZ13 and FZ10) in the SECS. Burial and thermal histories of Well FZ10 and the maturity simulation were analyzed in combination with findings of tectonic evolution using seismic interpretation results, paleogeotemperature gradient data, and R_o test data. In addition, the process of generating hydrocarbons from Lower–Middle Jurassic source rocks was determined. Based on this, the favorable accumulation models of oil–gas generated by Lower–Middle Jurassic source rock were proposed by combining analysis of elements and conditions of oil–gas accumulation.

4 Results

4.1 Comparison of Mesozoic tectonic environments and sedimentary strata between the NSCS and SECS

4.1.1 Geochemistry and age of Mesozoic igneous rocks

Xu et al. (2016) , Xu et al. (2017) studied the Mesozoic igneous rock samples that were found in more than 20 wells from the NSCS and more than 10 wells from the SECS. He observed a NE-SW trend belt of Early Jurassic (198–187 Ma) island arc igneous rocks from Shenhu Uplift–Panyu Uplift–Penghu Uplift in NSCS to Yandang Swell in the SECS, with low-potassium tholeiitic granite–diorite lithologies. This indicated that NSCS-SECS underwent the same tectonic environment at the beginning of the Jurassic. Moreover, Jurassic–Cretaceous I-type magmatic arc granites were recognized in the NSCS. The zircon U–Pb age had two peaks at 162–148 Ma and 137–102 Ma.

Zhang et al. (2019) and Si et al. (2021) tested granitoids in the SECS and Paleocene clastic rocks of the Lishui Depression. The results demonstrated that the zircon U–Pb age of the granitoids was 193–172 Ma and 115–111 Ma. Zircon has typical magmatic arc characteristics of fluid activity uranium (U) enrichment and high field intensity element (Nb) depletion. The zircon age of clastic rocks was Jurassic–Early Cretaceous, including three peaks of 194–184 Ma, 148–133 Ma, and 119–98 Ma. The age of the early clastic zircon peak (194–184 Ma) corresponded to the Early Jurassic igneous formation time proposed by Xu et al. (2016), Xu et al. (2017), while the late age peak (119–98 Ma) corresponded to the zircon age (137–102 Ma) of granitoids in the NSCS.

Overall, the wells in the NSCS-SECS revealed that the geochemical signature and age of Jurassic–Cretaceous igneous rocks were consistent, and both formed in the subduction-controlled magmatic arc environment of the East Asian Paleoplate.

4.1.2 Interpretation of geophysical data from the Early Jurassic magmatic belt

Zhou et al. (2005) recognized a NE trend (about 45°) subduction accretion zone in NSCS from the interpretation of gravity, magnetic, and wide-angle seismic data. This subduction accretion zone had an oblique intersection with current submarine topography and Cenozoic tectonic, indicating that it formed before the Cenozoic. In addition, this subduction accretion zone was shifted to the left by the NW trend fault forming an echelon, which agreed with the Mesozoic stress field. However, the time of formation of this subduction accretion zone was not discussed in this study. The Mesozoic subduction accretion zone would certainly cause strong tectonic movement and volcanism. The magmatic belt of Shenhu Uplift–Panyu Uplift–Penghu Uplift–Yandang Swell was presented by Xu et al. (2017), as a NE trend moniliform belt with low positive magnetic anomaly value on the map (Zhang et al., 2010). It extended from the NSCS to the SECS along a northeasterly direction, which corresponded to the northwest boundary of the Early–Middle Jurassic Basin. This magmatic belt was generally parallel to the Mesozoic subduction accretion zone proposed by Zhou et al. (2005). Therefore, it was proposed that this magmatic belt was also formed by plate subduction in this period. The interpretation of the igneous belt and the geochemical data can prove each other, which further confirmed that NSCS-SECS was in the same tectonic environment at the beginning of the Jurassic.

4.1.3 Basement properties and Mesozoic fracture

The basement of the Mesozoic Basin in the northern East China Sea was the extension of the Lower Yangtze Fold Belt toward the sea, while similar structures from the SECS to the NSCS (east side of the Yangjiang–Yitong'ansha fault) were the extension of the Caledonian Fold Belt in southern China toward the offshore (Lu et al., 2011; Sun et al., 2014). The basin basement in the NSCS-SECS was developed over the continental crust in a stable rigid basement. The basement of the Mesozoic Basin is regularly distributed.

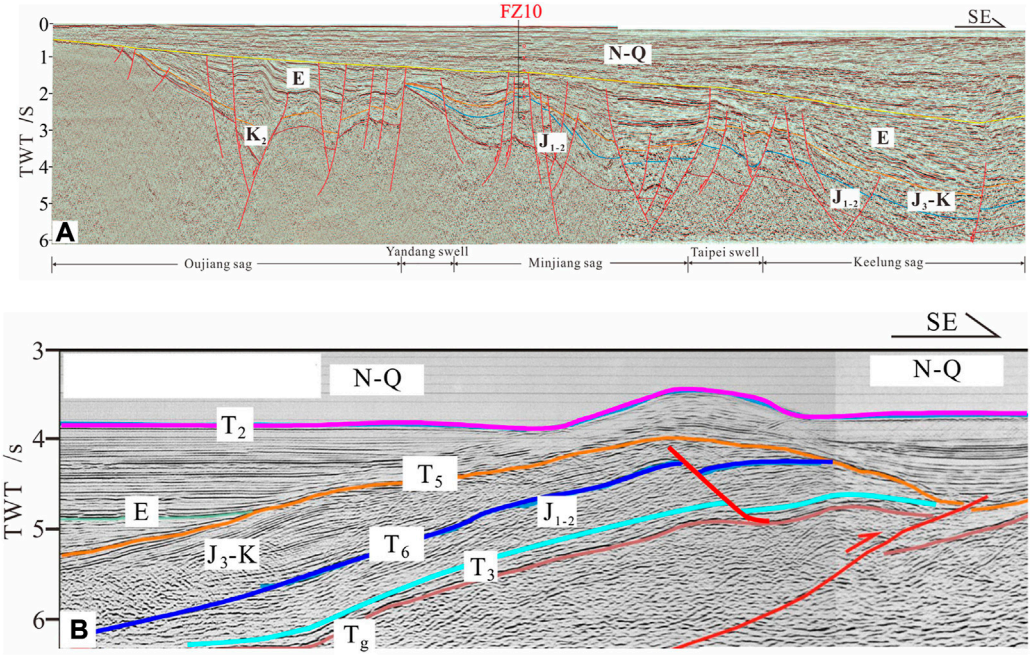

FIGURE 2
Seismic interpretation of SE oriented profiles showing the distribution of sedimentary strata along the SECS **(A)** and NSCS **(B)**. T_3 label represents the Late Triassic; J_{1-2} represents the Early–Middle Jurassic; J_3-K represents the Late Jurassic–Cretaceous; E represents the Paleocene; N-Q represents the Neocene–Quaternary; T_2 represents the boundary between the Neogene and Paleogene; T_5 represents the boundary between the Paleogene and Cretaceous; T_6 represents the boundary between the Late Jurassic and Middle Jurassic; and T_g represents the bottom boundary of the Mesozoic.

The bottom part is essentially formed by Presinian crystalline rocks (Li, 2001; Li et al., 2014; Sun et al., 2014; Li S. et al., 2018), and the lithological features discussed earlier were diverse in different basins. Specifically, the basement underlying Mesozoic sedimentary rocks in SECS was formed by Proterozoic metamorphic rocks, Mesozoic intrusive rocks, and acidic volcanic rocks (Li, 2001). The rocks of this basement along the West and southwest Taiwan basins are Late Paleozoic schist, marbles, and igneous (Liu et al., 2006; Li et al., 2014). The basement of the Pearl River Mouth Basin east of the Yangjiang–Yitong'ansha Fault was mainly formed by Early Jurassic granites and granodiorites (Liu et al., 2006; Li et al., 2014). The basement lithology can be compared with rocks in Zhejiang, Fujian, and Guangdong provinces sharing the same age (Wang et al., 2022b). Seismic, gravity, and magnetic data reveal that Mesozoic fractures with a NE and NW trend were developed from NSCS to SECS (Yi et al., 2012; Lu et al., 2015; Liu et al., 2019). Precisely, the NE trend was the main tectonic direction and was developed early, while the NW trend fault was developed slightly late and intersected by the NE trend fault (Figure 1), which was the left-lateral strike-slip fault (Sun et al., 2014; Xia et al., 2018). Faulting played an important role in adjusting the tectonic deformation in the area. The Mesozoic tectonic structure appears to be separated by those large basement faults in the NSCS-SECS with the characteristics of NE trend belts intersected by NW faults (Yi et al., 2012).

4.1.4 Jurassic–Cretaceous strata

There were extensive distributions of the Mesozoic formation from NSCS to SECS, with continuous and comparable lateral strata. In the Early–Middle Jurassic, there was stable marine sedimentation from NSCS to SECS, accompanied by a gradual reduction in the water depth and transition of sedimentary facies from bathyal–abyssal plain facies to littoral–neritic facies (Qiu and Wen, 2004). The Lower–Middle Jurassic (J_{1-2}) was a group of low to moderate amplitude, less continuous to continuous reflectors, external sheet-wedge, and parallel–sub-parallel internal structures in seismic profiles (Figure 2). The Lower–Middle Jurassic (J_{1-2}) in the basin was in conformable contact with the underlying Upper Triassic Series and in unconformable contact at the basin edges. The NSCS was mainly developed with Late Jurassic to Cretaceous bathyal and littoral–neritic facies, which were gradually transitioned to neritic, paralic, and continental facies in SECS. In seismic, the Upper Jurassic–Cretaceous (J_3-K) is interpreted as a set of mid–high amplitude, continuous lamellar reflectance, with external wedge, and

internal divergent structures (Figure 2). The top of Upper Jurassic–Cretaceous strata was often bare, which was an unconformable angular contact with the overlying Cenozoic strata.

4.2 Characteristics of the Jurassic source rock

The thickness of the Lower–Middle Jurassic succession from regional geological analysis and seismic data interpretation is approximately 1,500–4,000 m and the sedimentation center is at the Keelung Sag, with a thickness of 4,000 m. A comprehensive analysis of well and seismic data indicates that the water depth in the SECS gradually decreased from northwest to southeast, along which it developed with sedimentation of fluvial, paralic, neritic, and bathyal–abyssal facies. Jurassic dark mudstones are generally distributed to the northeast and the total thickness ranges from 100 to 700 m. The depocenter is in the mid-south of the Keelung Sag, which is about 600–800 m thick (Wang et al., 2019).

In the study area, wells FZ13 and FZ10 intersected Jurassic strata located eastward near the coast of the Panyu Uplift–Penghu Uplift–Yandang Swell (Figure 1). Coastal neritic dark mudstones and paralic facies coal seams are dominant in these two wells. The statistics of geochemical core data from these wells indicate that the organic carbon content of the dark mudstone is 0.69%–0.98%, reaching a maximum of 1.24%. Rock-Eval pyrolysis S1+S2 was between 0.63 and 1.97 mg/g. These dark mudstones were determined to be source rocks of moderate abundance. The organic content in carboniferous source rocks can reach 67%–75% and pyrolysis S1+S2 was between 155 and 169.6 mg/g, belonging to rich source rocks. Most of the organic matter in the Jurassic source rocks was type III and some reached type II. Type III source rocks are generally humic-type source rocks capable of generating gas.

Currently, no wells have been drilled at the Keelung Sag. Many wells in the west Taiwan Basin adjacent to the south of the study area revealed that abyssal plain shale was developed in the Lower and Middle Jurassic, with organic content ranging from 0.6% to 1.8%, compared to the surrounding strata in the same period. They can be good source rocks due to their high organic content (Qiu and Wen, 2004; Zhou et al., 2006). At the beginning of the Middle Jurassic, the water depth in the SECS gradually increased along the southeast and was mainly of medium–high amplitude, sub-parallel to parallel reflection in the seismic data, which has been identified as the stable sedimentation of the bathyal–abyssal facies (Yang et al., 2015; Yang et al., 2017; Wang et al., 2019). This was conducive to aggregation and accumulation of organic matter. Thus, we postulate that the Keelung Sag, which is the depocenter of Early–Middle Jurassic sedimentation, had good conditions for the generation of hydrocarbons.

4.3 Characteristics of the reservoir and seal rock

4.3.1 Mesozoic reservoir

Mesozoic reservoir data statistics from wells FZ13 and FZ10 suggest that the reservoir was composed mainly of sandstones and siltstones of coastal–neritic facies (Figure 3), and the reservoir pore spaces were mainly composed of primary porosity and secondary fractures. The porosity gradually decreased with an increasing depth, influenced by the compaction, cementation, and subsidence of clay minerals. Generally, the buried depth of 3,100 m can be used as a limit. The porosity above 3,100 m was higher than 10%, showing good accumulation properties. The porosity below 3,100 m decreased markedly and was mostly less than 10%, showing relatively low permeability. Overall, the porosity of Lower Jurassic sandstones was generally less than 10% due to compaction and diagenesis influences (Table 1). Current studies show that tectonism-controlled fracture development in tight reservoirs can significantly improve reservoir properties (Li et al., 2019; Fan et al., 2022; Li H. et al., 2022; Li J. et al., 2022). This evolved secondary pores and cracks in the sedimentary layers, leading to porosity enhancement. The porosity of the Upper Jurassic–Lower Cretaceous sandstone was generally between 15%–20% (Table 1). Porosity in the layers developed with secondary pores and cracks can exceed 20%. The porosity of the Upper Cretaceous sandstone is generally greater than 20%, showing good reservoir accumulation properties.

4.3.2 Cenozoic reservoir

Sandstone is the main reservoir rock type, from silt to gravel in terms of grain size. Moreover, fine-medium grain sandstone is dominant. The Eocene Pinghu and Oligocene Huaguang formations are the most important strata (Figure 3). The reservoir pore spaces are mainly primary pores, secondary pores, micropores, and microcracks. Among them, the primary pores have the greatest contribution and the microcracks connected different types of pores effectively, thus improving the pore permeability of the reservoir. The porosity of Cenozoic Paleogene reservoir is generally 10%–25% and permeability is mostly less than 1,000 mD. Both porosity and permeability are not related to the buried depth.

4.3.3 Seal rock

Analysis of the core data shows that the overlying Cenozoic strata in the SECS were mainly composed of mudstones (Figure 3). The abyssal plain, bathyal, and paralic facies were developed during the Lower–Middle Jurassic, accompanied by extensive development of thick mudstone layers. In particular, thick layers of mudstone and shale were well developed at the Keelung Sag, being the depocenter of sedimentation, which was not only the good source rock but also the excellent regional seal rock. Upper Cretaceous coastal and paralic facies mudstones

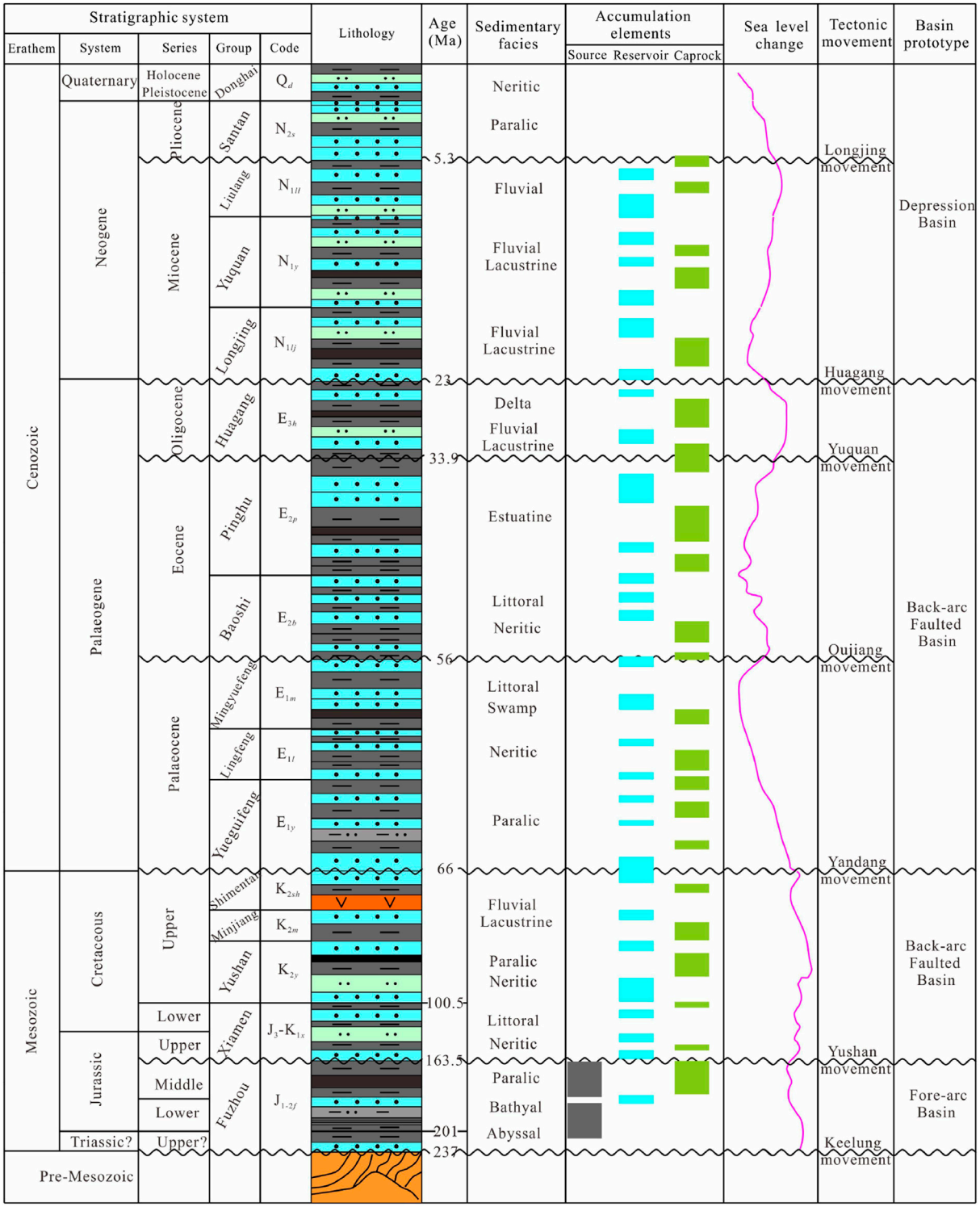

FIGURE 3
Stratigraphic chart of the SECS showing a combination of sedimentary facies, sea level changes, tectonic, and petroleum system since the Triassic (modified from Chen et al., 2016; Yang et al., 2012, 2017; Xiao et al., 2019; Wang et al., 2022a; as well as using drilling data of wells FZ10 and FZ13).

TABLE 1 Porosity distribution of the Mesozoic reservoir across wells FZ10 and FZ13 estimated from three strata (J, K_1, and K_2).

Strata	Porosity range (%)		Proportion of porosity<10% (%)		Proportion of porosity ranging 10%–15% (%)		Proportion of porosity ranging 15%–25% (%)		Proportion of porosity>25% (%)	
	FZ10	FZ13	FZ10	FZ13	FZ10	FZ13	FZ10	FZ13	FZ10	FZ13
K2	10.03–24.61	10.72–29.04	0	0	11.6	36.4	88.4	54.5	0	9.1
K1	7.76–19.99	4.09–22.64	21.9	55.6	58.9	31.7	19.2	12.7	0	0
J	5.78–12.67	5.8–8.97	75	100	25	0	0	0	0	0

have great thickness and extensive distribution and are good regional seal rocks. The Cenozoic regional seal rock mainly includes thick mudstones of neritic facies from the Paleocene Lingfeng Formation and the Eocene Baoshi Formation.

5 Discussion

5.1 Basin evolution since the Jurassic

Based on previous analysis, the NSCS-SECS was integrated and was a large unified basin during the Mesozoic. This basin extended to the northern Yandang Swell region of the East China Sea Basin as the northern boundary, the Yangjiang–Yitong'ansha Fault as the southwest boundary, and the Bijia Uplift–Diaoyu Island Fold Belt as the southeast boundary. It was separated from the mainland in the northwest by the Changle–Nan'ao Fault. This large basin has experienced consistent tectonic evolution since the Jurassic.

5.1.1 Fore-arc depression basin in the Early–Middle Jurassic

The study area has been controlled by the subduction of the Neo-Tethyls and Paleo-Pacific Plate into the Eurasian Plate since the Early Jurassic and the latter dominated. The Paleo-Pacific Plate melted and underwent metamorphic dehydration, accompanied by the NWW trend of low-angle progressive subduction from the Paleo-Pacific Plate to the Eurasian Plate (Li and Li, 2007; Li S et al., 2018), which induced the melting of the overlying continental crust of the obduction plate or the mantle wedge part (Li et al., 2017). Strong volcanism occurred along the Shenhu Uplift–Panyu Uplift–Penghu Uplift–Yandang Swell at the continental edges. Xu et al. (2017) demonstrated that these rocks had the geochemical characteristics of island arc igneous rocks. They were formed in the Early Jurassic based on the Zircon U–Pb age test. Hence, it can be postulated that the NSCS-SECS was in the Andes-type active continental margin stage for the development of the continental igneous arc. There was a fore-arc depression basin in front (southeast side) of the Panyu Uplift–Penghu Uplift–Yandang Swell igneous arc (Wang et al., 2022b) (Figure 4).

Figure 5 shows the balanced profile analysis in the SECS. The center of the strata's thickness was at the Keelung Sag and the eastern region of the Taibei Swell during the Early–Middle Jurassic. The strata were gradually thinned from the center of the basin to the northwest and southeast regions. The basin center was dominated by bathyal–abyssal facies, and the water depth decreased to the northwest and southeast. Meanwhile, the sedimentary facies transitioned into neritic and paralic facies.

5.1.2 Back-arc faulted basin in the Late Jurassic–Cretaceous

5.1.2.1 Late Jurassic–Early Cretaceous

The subduction direction from the Paleo-Pacific Plate to the Eurasian Plate changed to the NNW trend, in the Late Jurassic–Early Cretaceous, accompanied by an increase in the subduction angle (Suo et al., 2015; Li S. et al., 2018). The NSCS-SECS was in the left-lateral strike-slip extensional stress field environment (Sun et al., 2014; Xia et al., 2018). This was the peak stage of lithospheric thinning in eastern China, accompanied by strong fractures and volcanic activity. The lithology described from the well-core data was characterized by neutral-acid intrusive and eruptive rocks, belonging to I-type igneous arc granitoids. Most of the rocks contained common hornblendes and have enrichment of active fluid components and strong depletion of Ta-Nb-Ti. These were significantly different from I-type or A-type granites in South China at the same age. The Zircon U–Pb age had two peaks, which corresponded to twice strong Paleo-Pacific Plate subduction activities (Maruyama et al., 1997; Li et al., 1998; Xu et al., 2016; Xu et al., 2017; Yuan et al., 2018; Zhang et al., 2019). These rocks are mainly distributed in Dongsha Uplift, Shenhu Uplift, and Panyu Uplift in the NSCS and extended to the SECS. Furthermore, the rifting activity from the mainland to the offshore at the end of the Yanshan period and the cooling trend disclosed by the zircon/apatite fission track revealed that the Paleo-Pacific Plate had subduction retreat during 125–100 Ma (Suo et al., 2015; Li S et al., 2018). Balanced profile analysis showed that this stage was mainly

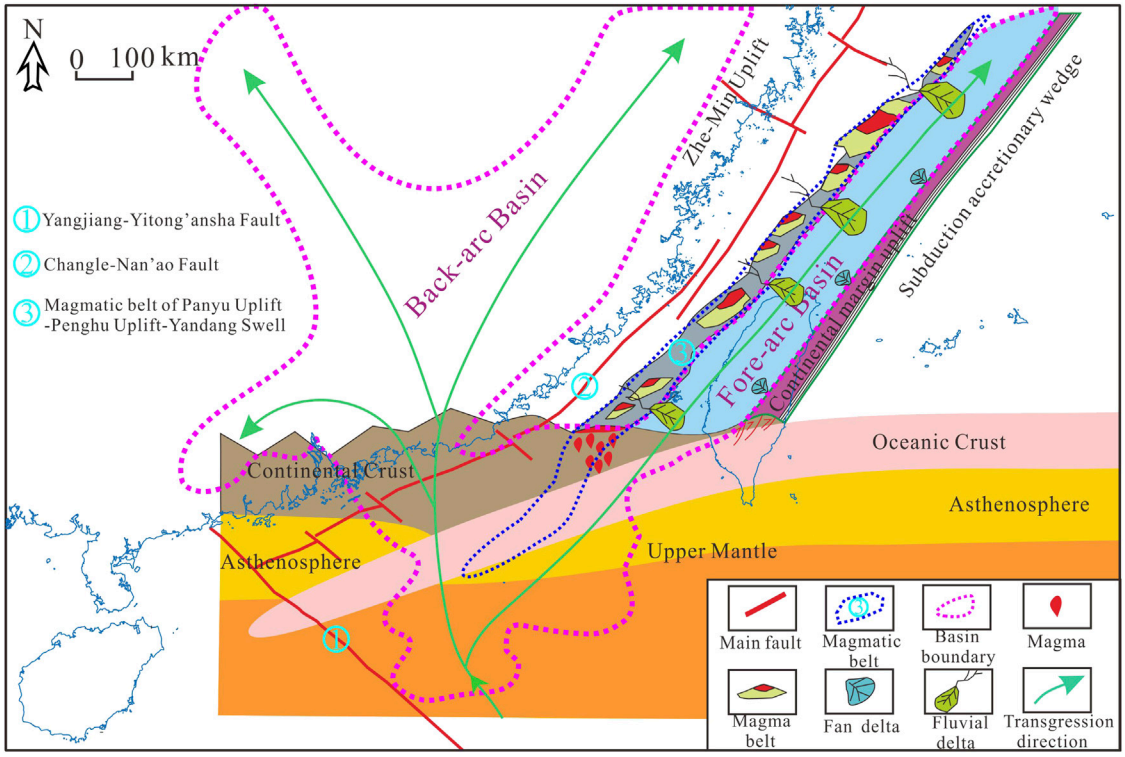

FIGURE 4
Plane view of the Early–Middle Jurassic Basin (pink dotted lines) and transgression direction (green arrow lines) in the NSCS-SECS, as well as the sedimentary system in the SECS. In the vertical section, we show the deep structural features, the magma activity, and the basin formation mechanism (modified from Zhou et al., 2005; Yi et al., 2012; Wu, 2014; Wang et al., 2022a; 2022b).

characterized by the development of NE trend boundary faults (e.g., western fault of Diaoyu Island which is shown in Figures 1, 5). Moreover, basin distribution and sedimentary strata were controlled by these boundary faults (Figure 5). In the Late Jurassic–Early Cretaceous, the NSCS-SECS was in the development stage of the back-arc faulted basin (Wang et al., 2022a; 2022b) (Figure 6). Water depth gradually increased from northwest to southeast and gradually evolved from continental to marine facies. The Keelung Sag was the depositional center at this stage, where it was primarily developed with bathyal–abyssal facies.

5.1.2.2 Late Cretaceous

Since the Late Cretaceous, the Pacific Plate replaced the Izanagi Plate (part of the Paleo-Pacific Plate) and was subducted into the NWW direction. Meanwhile, the Indian Plate began to move rapidly northward and collide with the Eurasian Plate (Xu et al., 2017). The ophiolite that was developed in eastern Taiwan, China, and the Philippines should be the remnant of the Late Mesozoic subducted oceanic crust (Dimalanta and Yumul, 2006; Dimalanta and Yumul, 2006; Asis and Jasin, 2012). The findings from studying lithology, chronology, and tectonic environment of igneous rocks over the same span period in coastal areas of southeast China (Chen et al., 2008; Hong, 2012), revealed that the lithology was mainly two-peak volcanic rocks (rhyolite/basalt) and A-type granite, which was formed in the regional extensional tectonic environment around 100–72 Ma (Ye, 2019). In the Late Cretaceous, the NSCS was in the weak tectonic belt under the interaction of the Pacific Plate, Eurasian Plate, and Indian Plate. A mantle plume was formed which extruded to the southeast and an NW-SE trending extensional stress field was generated. The NSCS area split to the southeast and a back-arc extensional faulted basin was formed. However, only a small-scaled retreat of the Pacific subduction zone occurred in SECS north of the weak tectonic belt. The SECS developed a faulted depression gradually eastward of the former Yandang old uplift. Compared with the earlier tectonic period, sedimentation of the basin was extended, but it was still a back-arc extensional faulted basin (Figure 7). This tectonic event corresponded to the Yandang Movement.

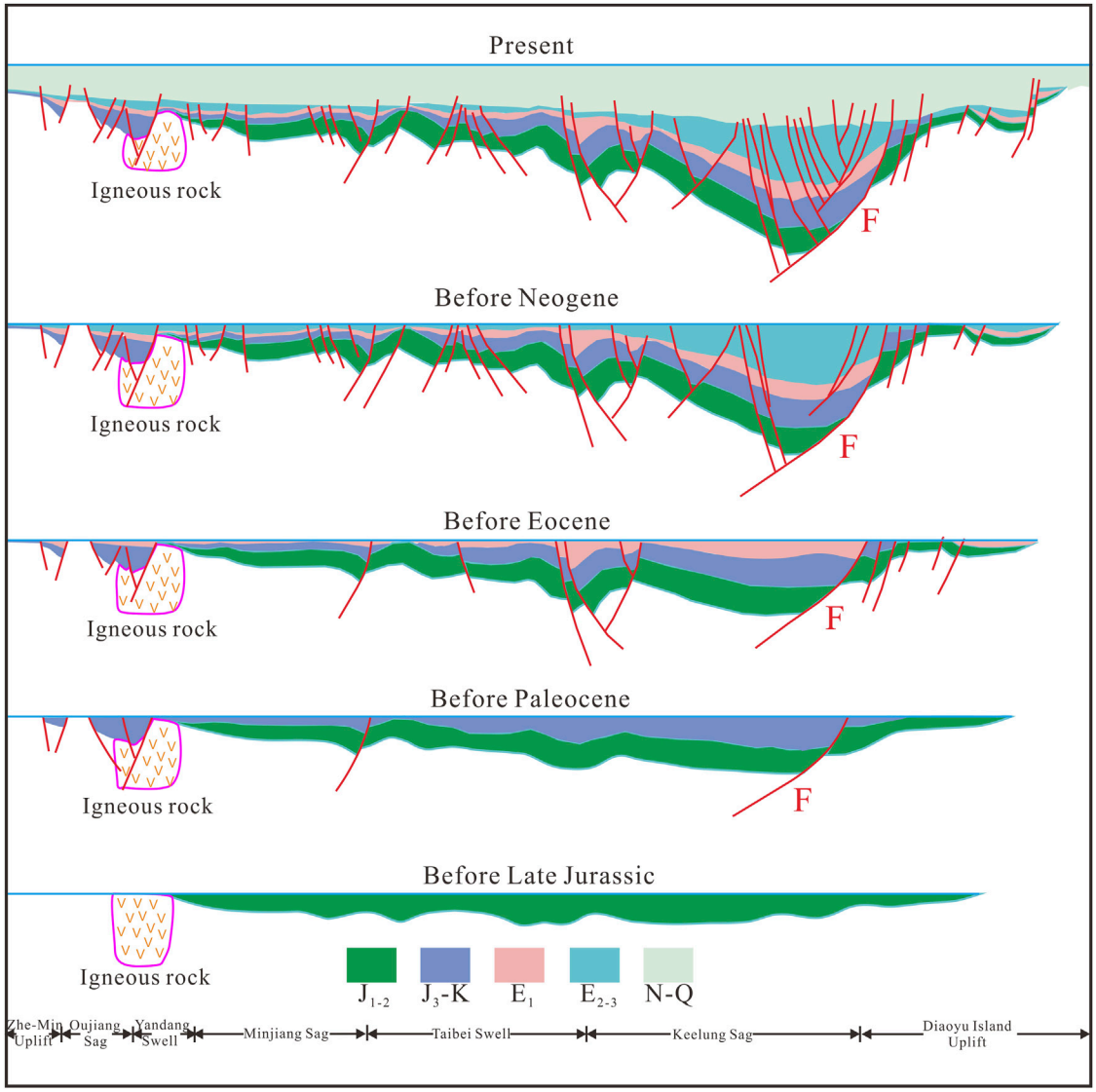

FIGURE 5
Tectonic evolution of SECS constructed from balanced section analysis in the southeast direction (F represents the western fault of Diaoyu Island in Figure 5). The J_{1-2} label represents the Early–Middle Jurassic; J_3-K represents the Late Jurassic–Cretaceous; E_1 represents the Paleocene; E_{2-3} represents the Eocene–Oligocene; and N-Q represents the Neocene–Quaternary.

5.2 Basin evolution since the Paleogene

Tectonic differential evolutionary characteristics in the NSCS-SECS have become increasingly prominent since the Paleogene, compared to before. Many scholars have studied the Cenozoic tectonic evolutionary process in the SECS and research results were consistent (Yang et al., 2012; Yang et al., 2017; Li et al., 2017; Zhong et al., 2018; Liu et al., 2020). The subduction influence of the Pacific Plate and the Philippine Sea Plate on SECS is more evident.

5.2.1 Paleogene back-arc faulted basin

In the Late Paleocene, the direction of motion of the Pacific Plate changed from NWW to NNW and SECS was in the simple shear stress field, thus resulting in a series of half-graben depression. This tectonic event corresponded to the Oujiang Movement. The direction of the Pacific Plate movement turned to the NWW at the end of the Eocene. Meanwhile, the Philippine Plate has begun to make NWW sloping subduction below the Eurasian Plate. The SECS underwent the tectonic event (Yuquan Movement) that was dominated by shear compression at the end of Eocene. In the Paleogene, the SECS was in a back-arc faulted

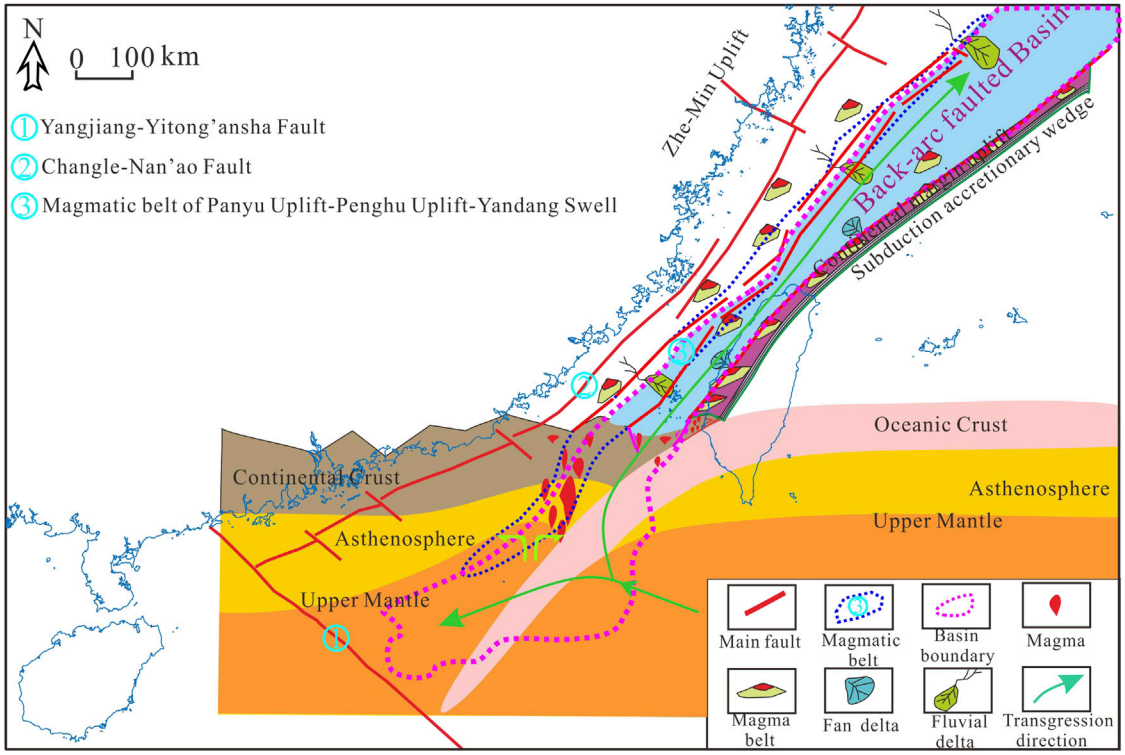

FIGURE 6
Plane view of the Late Jurassic–Early Cretaceous Basin (pink dotted line) and transgression direction (green arrow lines) in the NSCS-SECS, as well as the sedimentary system in the SECS. In the vertical section, we show the deep structural features, the magma activity, and the basin formation mechanism (modified from Zhou et al., 2005; Yi et al., 2012; Wu, 2014; Wang et al., 2022a; 2022b).

basin evolution stage, characterized by faults to the east and overlaps to the west. The center of early sedimentation was in the faulted Oujiang depression and the center of late sedimentation migrated eastward to the Keelung Sag, with characteristics of thick in the east and thin in the west. There were clastic rocks developed in paralic, neritic, and abyssal facies.

5.2.2 Neogene–Quaternary depression basin

There was little rifting development in the SECS from Neogene to the Quaternary, which was the evolutionary stage of thermal subsidence, followed by sedimentary deposition of fluvial, alluvial plain, and marine facies, with high strata thickness to the east and low to the west. Although this stage was relatively stable, there were still under tectonic events. In the Middle and Late Miocene, the Philippine Plate accelerated to assembly toward the Eurasian Plate and the regional stress field changed from the dextral slip transtension to sinistral slip transpression (Suo et al., 2015). The SECS underwent uplifting extrusion. The Oligocene–Lower Miocene strata are missing in the western depression of the basin due to denudation, marginal sea closure, and structural inversion (Zhou, 2002). This event corresponded to the Longjing Movement.

5.3 Hydrocarbon generation of the Jurassic source rocks

The SECS has experienced multiple stages of tectonic deformation since the Jurassic. The Lower–Middle Jurassic source rocks experienced multiple stages of uplift and burial, which corresponded to various stages of hydrocarbon generation. Well FZ10 was on the western edge of the NSCS-SECS Mesozoic Basin, and the buried depth of Lower–Middle Jurassic source rocks was relatively shallow. The R_o of the Lower–Middle Jurassic dark mudstones, in most samples, ranged between 0.65% and 0.78% and the source rocks were mature. From the single-well burial history and thermal evolution of FZ10 (Figure 8), the Lower–Middle Jurassic source rocks started generating hydrocarbons since the Late Paleocene and ceased in the Oligocene due to the tectonic uplift. The SECS subsided again

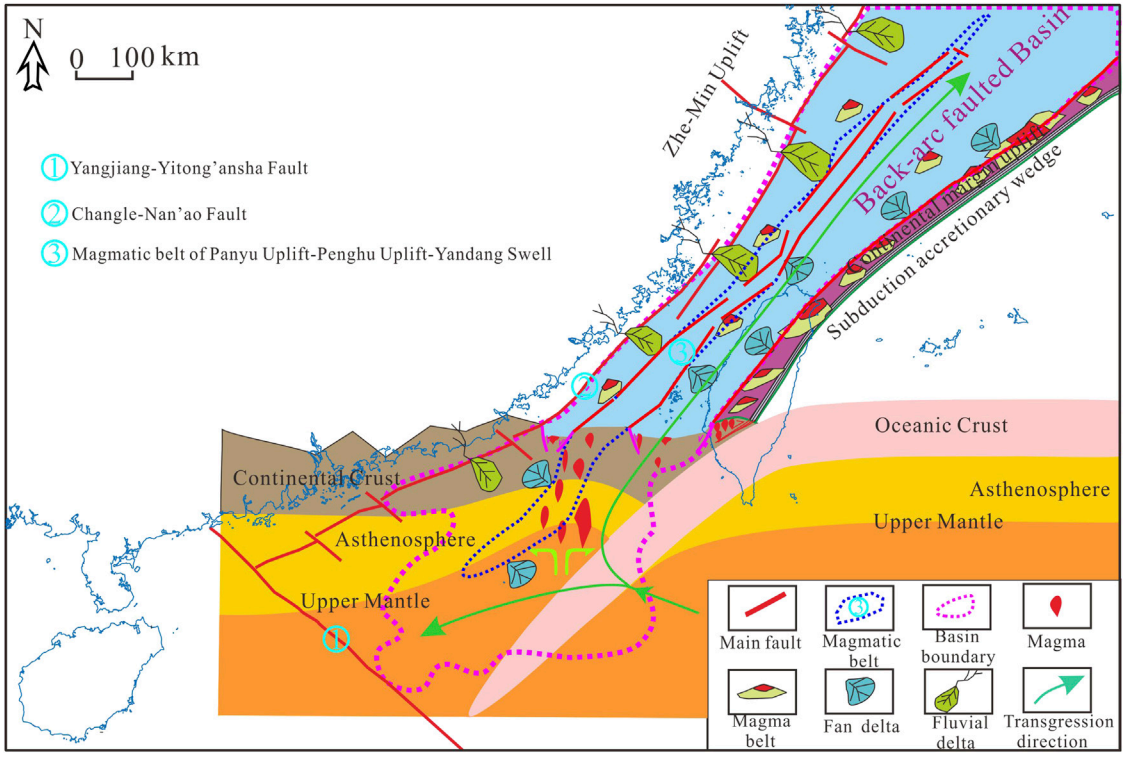

FIGURE 7
Plane view of the Late Cretaceous Basin (pink dotted line) and transgression direction (green arrow lines) in the NSCS-SECS, as well as the sedimentary system in the SECS. In the vertical section, we show the deep structural features, the magma activity, and the basin formation mechanism (modified from Zhou et al., 2005; Yi et al., 2012; Wu, 2014; Wang et al., 2022b).

in Neogene, reactivating the Lower–Middle Jurassic source rocks to another stage of hydrocarbon generation.

Thermal maturity analysis indicates that the Keelung Sag became the depocenter of the Lower–Middle Jurassic source rocks. Our results of seismic data interpretation were used for well simulation chosen to analyze the burial history of the Keelung Sag (Figure 9). The Lower–Middle Jurassic source rocks at the Keelung Sag reached maturity stage in the Late Jurassic and hydrocarbon generation was interrupted in the early Late Cretaceous due to the tectonic uplift. Hydrocarbon generation was reactivated after the heat flow reached the maximum temperature again and lasted until the Late Oligocene when another uplift stage occurred. The Keelung Sag is believed to have entered another thermal subsidence stage after Neogene. As the buried depth increased, the source rocks returned to generate hydrocarbons since then. The Lower–Middle Jurassic dark mudstones were deposited at the Keelung Sag and generated oil and gas that could migrate and accumulate in reservoirs along the western Taibei Turning zone and high topographic zones in other regions.

5.4 Jurassic oil–gas migration and accumulation model

Paralic and littoral facies sedimentation with good porosity sand bodies occurred in the SECS from the Upper Jurassic-Cretaceous and Paleogene systems. Oil and gas generated by Lower–Middle Jurassic source rocks can migrate through these sand bodies. Yushan Movement occurred in the end of the Middle Jurassic. The SECS entered the back-arc faulted basin development stage and formed some faults. The Yandang Movement in the Late Cretaceous was an extensional regime, during which abundant normal faults were developed, accompanied by extensive volcanism. The Huagang Movement occurred in the Late Paleogene and was a compressive shear tectonic movement, with weak tectonic deformation and no-fault development. This mainly induced regional uplift and denudation in the SECS, and the local tectonic was further shaped. The regional unconformities formed by the Yushan, Yandang, and Huagang movements were important pathways for oil–gas lateral migration. In addition, there were several

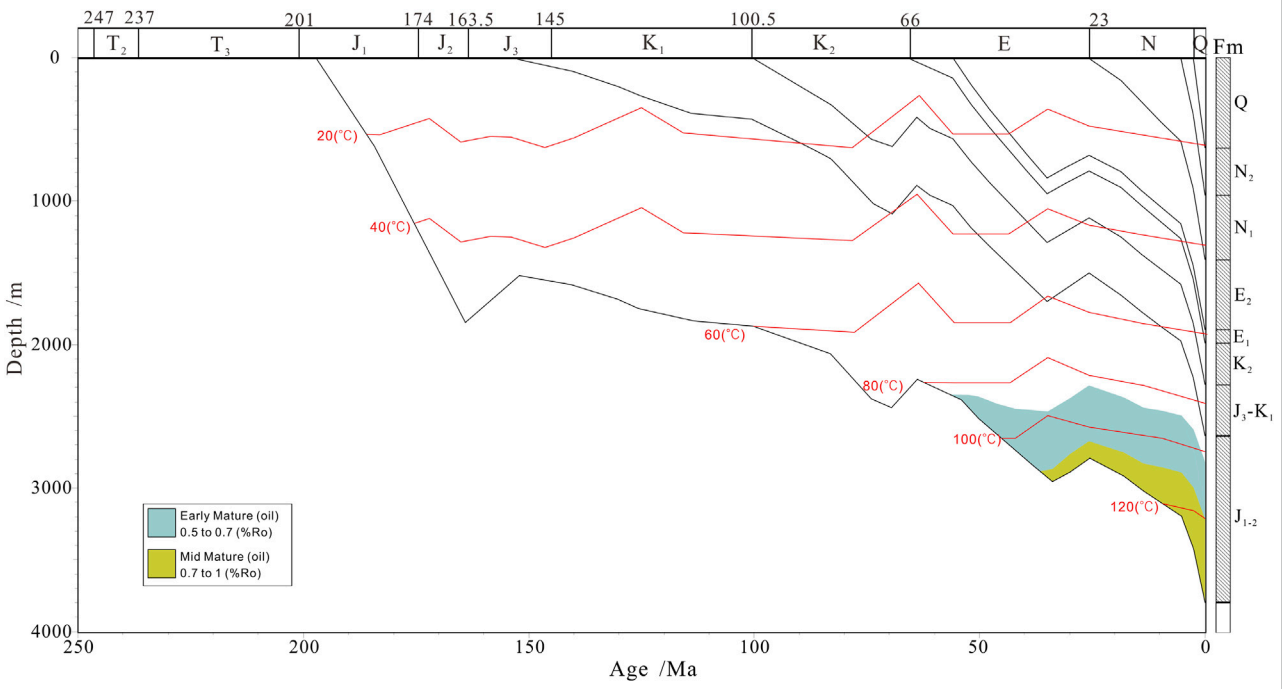

FIGURE 8
Burial history and thermal evolution of the Well FZ10 (location is shown in Figure 1). The fill colors represent different stages of maturity evolution. The J_{1-2} label represents the Early–Middle Jurassic; J_3-K_1 represents the Late Jurassic–Early Cretaceous; K_2 represents the Late Cretaceous; E_1 represents the Paleocene; E_2 represents the Eocene; N_1 represents the Miocene; N_2 represents the Pliocene; and Q represents the Quaternary.

local conformities in the region, which were also conducive to lateral oil and gas migration.

Figure 10 illustrates the combination of hydrocarbon generation, accumulation and seal rock, as well as oil–gas migration characteristics in the SECS. The oil–gas accumulation model of the Lower–Middle Jurassic source rocks is shown in Figure 11.

The process of generating hydrocarbons in different tectonic units differs significantly in the study area. This process becomes more complicated from the basin edges to the Keelung Sag, which was the depocenter of sedimentation. Well FZ10 was drilled on the edge of the large Mesozoic East China Sea Basin. The thermal evolution level of the Lower–Middle Jurassic source rocks was relatively low and only experienced two stages of hydrocarbon generation at the Middle Paleogene and Neogene–Present. The burial history diagram at the Keelung Sag suggests that the thermal evolution level of the Lower–Middle Jurassic source rocks was high and experienced three stages of hydrocarbon generation in the Early Cretaceous–mid Late Cretaceous, Middle Paleogene, and Neogene–Present. In addition, the Lower–Middle Jurassic source rocks at the Keelung Sag were the hydrocarbon generation center in the SECS associated with the high organic content, good kerogen types, and great thickness. The SECS entered the hydrocarbon generation stage during the first development stage of the back-arc faulted basin in the Early Cretaceous–mid Late Cretaceous vertical and lateral oil–gas migration generated by Lower–Middle Jurassic source rocks were relatively active, which formed mainly Mesozoic fault block, and lithologies forming oil–gas reservoirs (Figure 11). Faults with positive structures evolved during the second development stage of the back-arc faulted basin in the Middle Paleogene. Faults intersected the Lower–Middle Jurassic source rocks and affected the oil–gas reservoir formed in the early stage. Oil and gas generated from the Lower–Middle Jurassic source rocks can migrate into shallow traps and accumulate in reservoirs along faults, unconformities, and sand bodies, which formed mainly Mesozoic–Cenozoic reservoirs created by fault blocks and, combination of structural and stratigraphical compounds (traps) (Figure 11). The depression-forming basin stage occurred during the Neogene, which was characterized by integral uplift or subsidence. Tectonic activities were weak. The oil and gas generated by the Lower–Middle Jurassic source rocks lacked good migration pathways, which accumulated in the reservoirs of the surrounding traps (Figure 11).

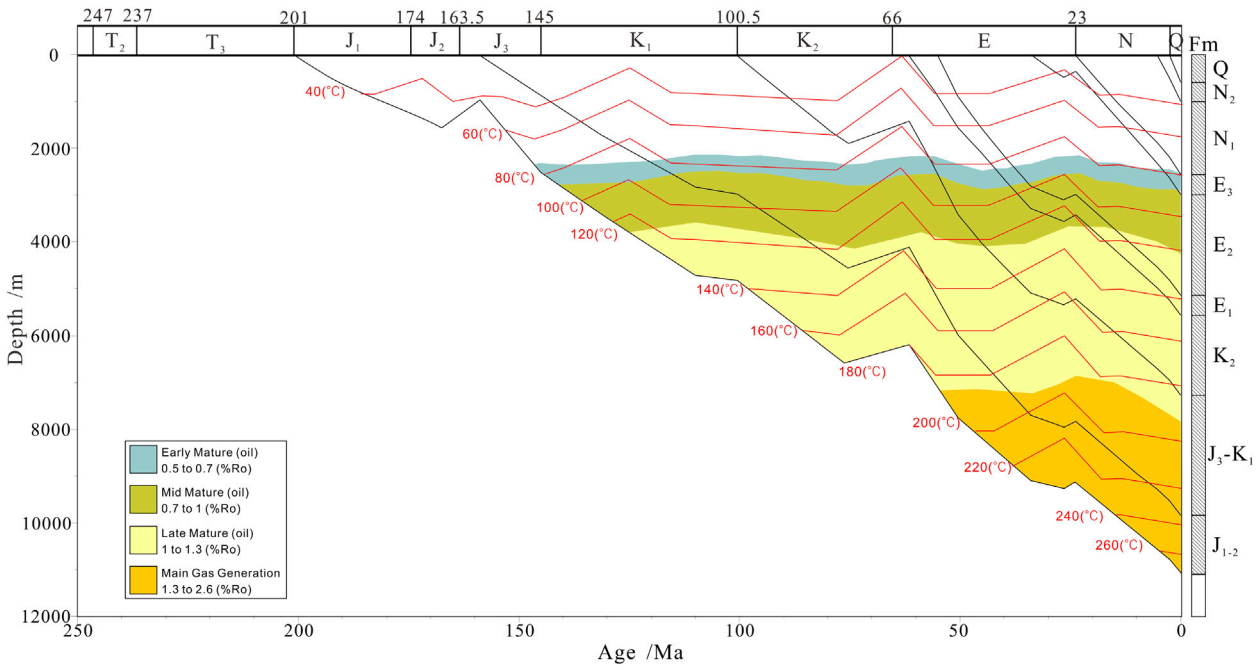

FIGURE 9
Burial history and thermal evolution at the Keelung sag (well location is shown in Figure 1). The fill colors represent different stages of maturity evolution. The $J_{1\text{-}2}$ label represents the Early–Middle Jurassic; J_3-K_1 represents the Late Jurassic–Early Cretaceous; K_2 represents the Late Cretaceous; E_1 represents the Paleocene; E_2 represents the Eocene; E_3 represents the Oligocene; N_1 represents the Miocene; N_2 represents the Pliocene; and Q represents the Quaternary.

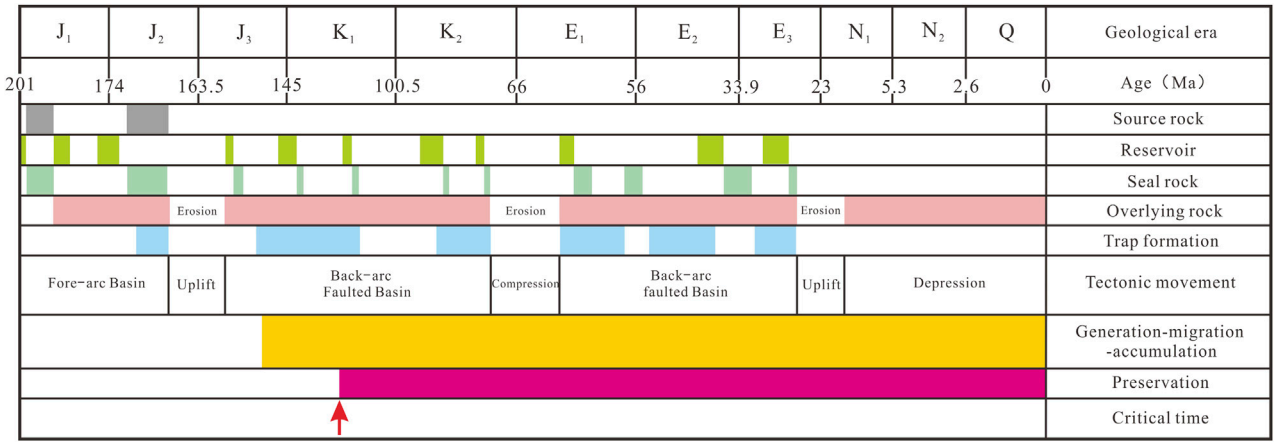

FIGURE 10
Petroleum system event chart summarizes the Jurassic oil-gas accumulation elements and processes at the Keelung Sag. The J_1 label represents the Early Jurassic; J_2 represents the Middle Jurassic; J_3 represents the Late Jurassic K_1 represents the Early Cretaceous; K_2 represents the Late Cretaceous; E_1 represents the Paleocene; E_2 represents the Eocene; E_3 represents the Oligocene; N_1 represents the Miocene; N_2 represents the Pliocene; and Q represents the Quaternary.

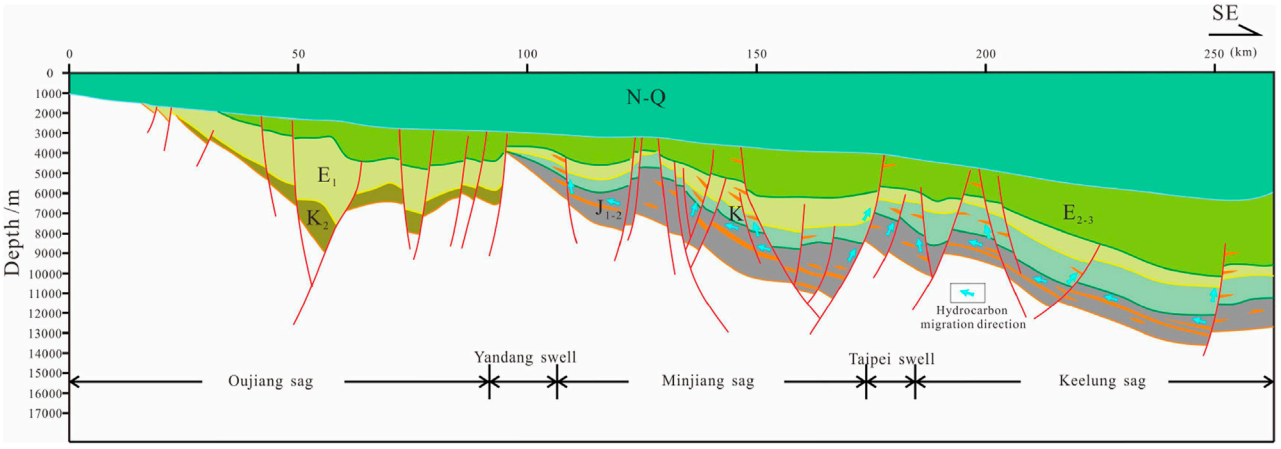

FIGURE 11
Favorable Jurassic oil-gas accumulation models in the SECS (location of the Section C is shown in Figure 1). The fill colors represent different strata. The J_{1-2} label represents the Early–Middle Jurassic; J_3-K represents the Late Jurassic–Cretaceous; K_2 represents the Late Cretaceous; E_1 represents the Paleocene; E_{2-3} represents the Eocene–Oligocene; and N-Q represents the Neogene–Quaternary.

6 Conclusion

(1) The NSCS-SECS was generally a large sedimentary basin during the Jurassic–Cretaceous period, which experienced two evolutionary stages from the Early–Middle Jurassic (J_{1-2}) fore-arc depression basin, to the Late Jurassic–Cretaceous (J_3-K) back-arc faulted basin. The NSCS-SECS entered the differential evolution process since the Cenozoic.

(2) The Keelung Sag in the SECS experienced three stages of hydrocarbon generation controlled by tectonic evolution in the Early Cretaceous–mid Late Cretaceous, Middle Paleogene, and Neogene–Present. However, other regions experienced only two stages of hydrocarbon generation. The Lower–Middle Jurassic source rocks at the Keelung Sag have a great thickness, high organic content, good kerogen type, and high thermal evolution level. It was the hydrocarbon generation center in the SECS.

(3) Oil and gas generated by the Lower–Middle Jurassic source rocks at the Keelung Sag migrated and accumulated in the western high tectonic traps along favorable sand bodies, unconformities, fractures, and pathways. It was the faulted basin including two rifting stages, in the Early Cretaceous–middle Late Cretaceous and Middle Paleogene. Active fault migration occurred, mainly forming Mesozoic–Cenozoic fault blocks and tectonic–lithological oil–gas reservoir. The study area remains in the depression basin development stage since the Neogene. The tectonic activities were weak and the oil and gas generated by the source rocks accumulated mainly in the surrounding traps.

Data availability statement

The original contributions presented in the study are included in the article/Supplementary Material; further inquiries can be directed to the corresponding authors.

Author contributions

MW: substantial contributions to the conception and design of the work and writing of the original draft. XJ: evaluation of source rocks; establishment of the burial model; and review and editing. BL: interpretation of the seismic section; writing—review and editing; and supervision. LH: substantial contributions to the conception and design of the work and writing—review and editing. JP: tectonic evolution analysis. All persons who have made substantial contributions to the work reported in the manuscript, including those who provided editing and writing assistance but who are not authors, are named in the Acknowledgments section of the manuscript.

Funding

This study was financially supported by the geological survey program of China Geological Survey (DD20221710, DD20160137, and DD20190208), earthquake science and technology spark program of the China Earthquake Administration (XH22014A), and the National Natural Science Foundation of China (41606079).

Acknowledgments

The authors would like to thank the reviewers who gave many constructive suggestions on the manuscript. They would like to express their gratitude to EditSprings (https://www.editsprings.cn) for the expert linguistic services provided.

Conflict of interest

The authors declare that the research was conducted in the absence of any commercial or financial relationships that could be construed as a potential conflict of interest.

The reviewer LH declared a shared affiliation with the author MW to the handling editor at the time of review.

Publisher's note

All claims expressed in this article are solely those of the authors and do not necessarily represent those of their affiliated organizations, or those of the publisher, the editors, and the reviewers. Any product that may be evaluated in this article, or claim that may be made by its manufacturer, is not guaranteed or endorsed by the publisher.

References

Asis, J., and Jasin, B. (2012). Aptian to turonian radiolaria from the darvel bay ophiolite complex, kunak, sabah, kunak, sabah. *Bull. Geol. Soc. Malays.* 58, 89–96. doi:10.7186/bgsm58201213

Chen, C. H., Lee, C. Y., Lu, H. Y., and Hsieh, P. S. (2008). Generation of late cretaceous silicic rocks in SE China: Age, major element and numerical simulation constraints. *J. Asian Earth Sci.* 31 (4-6), 479–498. doi:10.1016/j.jseaes.2007.08.002

Chen, L., Guo, F., Steel, R. J., and Li, Y. (2016). Petrography and geochemistry of the late cretaceous redbeds in the Gan-hang belt, southeast China: Implications for provenance, source weathering, and tectonic setting. *Int. Geol. Rev.* 58 (10), 1196–1214. doi:10.1080/00206814.2016.1141378

Dimalanta, C. B., and Yumul, G. P. (2006). Magmatic and amagmatic contributions to crustal growth in the Philippine island arc system: Comparison of the Cretaceous and post-Cretaceous periods. *Geosci. J.* 10 (3), 321–329. doi:10.1007/BF02910373

Fan, C., Xie, H., Li, H., Zhao, S., Shi, X., Liu, J., et al. (2022). Complicated fault characterization and its influence on shale gas preservation in the southern margin of the sichuan basin, China, *Lithosphere*, 2022. 8035106. doi:10.2113/2022/8035106

Hong, W. T. (2012). *Research on the cretaceous bimodal volcanic rocks at yunshan Caldera,Yongtai county, fujian province*. Nanjing: Nanjing University.

Li, S., Wang, Y., and Wu, S. (2018). Meso-cenozoic tectonothermal pattern of the Pearl River Mouth basin: Constraints from zircon and apatite fission track data. *Earth Sci. Front. Univ. Geosciences(Beijing); Peking Univ.* 25 (1), 95–107. doi:10.13745/j.esf.yx.2017-5-20

Li, G., Gong, J., Yang, C., Yang, C., Wang, W., Wang, H., et al. (2012). Stratigraphic features of the Mesozoic "Great east China sea"-A new exploration field. *Mar. Geol. Quat. Geol.* 32 (3), 97–104. doi:10.3724/SP.J.1140.2012.03097

Li, H., Zhou, J., Mou, X., Guo, H., Wang, X., An, H., et al. (2022). Pore structure and fractal characteristics of the marine shale of the longmaxi formation in the changning area, southern sichuan basin, China. *Front. Earth Sci.* 10, 1018274. doi:10.3389/feart.2022.1018274

Li, H., Tang, H., Qin, Q., Zhou, J., Qin, Z., Fan, C., et al. (2019). Characteristics, formation periods and genetic mechanisms of tectonic fractures in the tight gas sandstones reservoir: A case study of xujiahe formation in YB area, sichuan basin, China. *J. Pet. Sci. Eng.* 178, 723–735. doi:10.1016/j.petrol.2019.04.007

Li, J., Li, H., Yang, C., Wu, Y., Gao, Z., and Jiang, S. (2022). Geological characteristics and controlling factors of deep shale gas enrichment of the Wufeng-Longmaxi Formation in the southern Sichuan Basin, China. *Lithosphere* 2022, 4737801. doi:10.2113/2022/4737801

Li, J., Qi, B., Xu, H., Liu, X., and Yang, T. (2014). Cenozoic tectonic evolution of Wuqiuyu depression, Taixi basin. *Mar. Geol. Front.* 30 (9), 36–42. doi:10.16028/j.1009-2722.2014.09.016

Li, P., Liang, H., and Dai, Y. (1998). Exploration perspective of basement hydrocarbon accumulations in the Pearl River Mouth basin. *China Offshore Oil Gas* 12 (6), 361–369.

Li, S., Zang, Y., Wang, P., Suo, Y., Li, X., Liu, X., et al. (2017). Mesozoic tectonic transition in South China and initiation of Palaeo-Pacific subdcution. *Earth Sci. Front. Univ. Geosciences(Beijing); Peking Univ.* 24 (4), 213–225. doi:10.13745/j.esf.yx.2017-4-13

Li, W. (2001). Oil and gas prospects for the multicycle composite basin in the east China sea shelf. *Petroleum Geol. Exp.* 23 (2), 141–145. doi:10.11781/sysydz200102141

Li, S., Suo, Y., Li, X., Wang, Y., Cao, X., Wang, P., et al. (2018). Mesozoic plate subduction in West Pacific and tectono-magmatic response in the East Asian ocean-continent connection zone. *Chin. Sci. Bull.* 63 (16), 1550–1593. doi:10.1360/n972017-01113

Li, Z. X., and Li, X. H. (2007). formation of the 1300-km-wide intracontinental orogen and post orogenic magmatic province in mesozoic south China: A flat-slab subduction model. *Geol.* 35 (2), 179–182. doi:10.1130/G23193A.1

Liu, J., Xu, H., Jiang, Y., Wang, J., and He, X. (2020). Mesozoic and Cenozoic basin structure and tectonic evolution in the East China Sea basin. *ACTA Geol. SIN.* 94 (3), 675–691. doi:10.19762/j.cnki.dizhixuebao.2020115

Liu, Y., Wu, Z., Chen, Y., Wu, K., He, M., Zhang, J., et al. (2019). Spatial and temporal difference of Paleogene rift structure and its controlling factors in the northern South China sea: A case study of Pearl River Mouth basin. *J. China Univ. Min. Technol.* 48 (2), 367–376. doi:10.13247/j.cnki.jcumt.000933

Liu, Z., Wang, Y., Deng, A., and Gao, H. (2006). Petroleum geological characteristics and petroleum system of Taiwan strait basin. *Petroleum Geol. Exp.* 28 (6), 523–528. doi:10.3969/j.issn.1001-6112.2006.06.004

Lu, B., Sun, X., Zhang, G., Zhang, B., Lang, Y., and Wang, P. (2011). Seismic-potential field response characteristics and identification of basement lithology of the northern South China Sea basin. *Chin. J. Geophys.* 54 (2), 563–572. doi:10.3969/j.issn.0001-5733.2011.02.036

Lu, B. L., Wang, P. J., Zhang, G. C., and Wang, W. Y. (2015). Characteristic of regional fractures in South China Sea and its basement tectonic framework. *Prog. Geophys.* 30 (4), 1544–1553. doi:10.6038/pg20150408

Maruyama, S., Isozaki, Y., Kimura, G., and Terabayashi, M. (1997). Paleogeographic maps of the Japanese Islands: Plate tectonic synthesis from 750 Ma to the presentPaleogeographic maps of the Japanese Islands: Plate tectonic synthesis from 750 Ma to the present. *Isl. Arc* 6 (1), 121–142. doi:10.1111/j.1440-1738.1997.tb00043.x

Qiu, Y., and Wen, N. (2004). Mesozoic of the South in the area of the China eastern sea Sea and its significance northern margin for oil/gas exploration. *Geol. Bull. China* 23 (2), 142–146. doi:10.3969/j.issn.1671-2552.2004.02.007

Si, Q., Xu, C., and Gao, S. (2021). Late Mesozoic magmatic arc of East China Sea developed with plate subduction:constraints from detrital zircons in well FZ211. *Acta Geol. Sin.* 95 (6), 1743–1753. doi:10.19762/j.cnki.dizhixuebao.2020093

Sun, J., Yang, C., Wang, J., and Han, B. (2017). Tectonic evolution of the Jilong Sag and its petroleum potential. *Mar. Geol. Front.* 33 (4), 38–42. doi:10.16028/j.1009-2722.2017.04006

Sun, X., Zhang, X., Zhang, G., Lu, B., Yue, J., and Zhang, B. (2014). Texture and tectonic attribute of Cenozoic basin basement in the northern South China Sea. *Sci. China Earth Sci.* 57, 1199–1211. doi:10.1007/s11430-014-4835-2

Suo, Y. H., Li, S. Z., Zhao, S. J., Somerville, I. D., Yu, S., Dai, L. M., et al. (2015). Continental margin basins in east asia: Tectonic implications of the meso-cenozoic east China sea pull-apart basins. *Geol. J.* 50 (2), 139–156. doi:10.1002/gj.2535

Wang, M., Pan, J., Gao, H., Huang, L., and Li, X. (2022a). Mesozoic basin evolution and hydrocarbon potential in north South China Sea and south East

China Sea. *Earth Sci. Front. Univ. Geosciences(Beijing); Peking Univ.* 29 (2), 1–9. doi:10.13745/j.esf.sf.2021.7.8

Wang, M. J., Xiao, G. L., Yang, C. Q., Yang, C. Q., Chen, X., and Huang, L. (2019). Characteristics and evaluation of Mesozoic source rocks in the southeastern East China Sea continental shelf. *China Geol.* 1 (2), 133–141. doi:10.31035/cg2018079

Wang, M., Xu, Y., Huang, L., Pan, J., and Li, X. (2022b). *Strata in east China sea and adjacent areas*. Beijing, China: Geological Publishing House.

Wang, M., Zhang, Y., Pan, J., Huang, L., Chen, X., Luo, D., et al. (2020). Geological structure of the large section in eastern China's sea areas and its constraint on comprehensive stratigraphic division. *Geol. China* 47 (5), 1474–1485. doi:10.12029/gc20200513

Wu, S. (2014). *Depositional process for the mesozoic epicontinental marine basin in northern South China sea*. Chengdu: Chengdu University of Technology.

Xia, L., Lin, C., Li, X., and Hu, Y. (2018). Characteristics of fault structures in Pearl River Mouth basin and control effect of them on sedimentary basin. *J. Xi'an Shiyou Univ. Nat. Sci. Ed.* 33 (5), 1–18. doi:10.3969/j.issn.1673-064X.2018.05.001

Xiao, G., Wang, M., Yang, C., and Pang, Y. (2019). Numerical simulation of Mesozoic hydrocarbon generation, migration and accumulation in the southern East China Sea. *Mar. Geol. Quat. Geol.* 39 (6), 138–149. doi:10.16562/j.cnki.0256-1492.2019070304

Xu, C., Shi, H., Barnes, C. G., and Zhou, Z. (2016). Tracing a late Mesozoic magmatic arc along the Southeast Asian margin from the granitoids drilled from the northern South China Sea. *Int. Geol. Rev.* 58 (1), 71–94. doi:10.1080/00206814.2015.1056256

Xu, C., Zhang, L., Shi, H., Brix, M. R., Huhma, H., Chen, L., et al. (2017). Tracing an early jurassic magmatic arc from south to east China seas. *Tectonics* 36, 466–492. doi:10.1002/2016TC004446

Yang, C., Han, B., Yang, Y., Yang, C., Sun, J., Yan, Z., et al. (2017). Oil and gas exploration in the mesozoic of east China Sea shelf basin: Progress and challenges. *Mar. Geol. Front.* 33 (4), 1–8. doi:10.16028/j.1009-2722.2017.04001

Yang, C., Li, G., Gong, J., and Yang, C. (2015). Petroleum geological conditions and exploration prospect of the mesozoic in southeast China sea area. *J. Jilin Univ. Earth Sci. Ed.* 15 (1), 1–12. doi:10.13278/j.cnki.jjuese.201501101

Yang, C., Yang, C., Li, G., Liao, J., and Gong, J. (2012). Mesozoic tectonic evolution and prototype basin characteristics in the southern East China Sea Shelf Basin. *Mar. Geol. Quarternary Geol.* 32 (3), 105–111. doi:10.3724/SP.J.1140.2012.03105

Yang, C., Yang, Y., Yang, C., Sun, J., Wang, J., Xiao, G., et al. (2019). Tectono-sedimentary evolution of the mesozoic in the southern East China Sea shelf basin and its bearing on petroleum exploration. *Mar. Geol. Quat. Geol.* 39 (6), 30–40. doi:10.16562/j.cnki.0256-1492.2019070305

Ye, Q. (2019). *The late mesozoic structure systems in the northern South China sea margin: Geodynamics and their influence on the cenozoic structures in the Pearl River Mouth basin*. Wuhan: China uviversity of Geosciences.

Yi, H., Zhang, L., and Lin, Z. (2012). Mesozoic tectonic framework and basin distribution characteristics of northern margin of South China Sea. *Petroleum Geol. Exp.* 34 (4), 388–394. doi:10.3969/j.issn.1001-6112.2012.04.008

Yuan, W., Yang, Z., Zhao, X., Santosh, M., and Zhou, X. (2018). Early jurassic granitoids from deep drill holes in the east China Sea basin: Implications for the initiation of palaeo-pacific tectono-magmatic cycle. *Int. Geol. Rev.* 60 (7), 813–824. doi:10.1080/00206814.2017.1351312

Zhang, C., Xu, C., He, M., and Gao, S. (2019). Late mesozoic convergent continental margin with magmatic arc from east to south China seas: A review. *Adv. Earth Sci.* 34 (9), 950–961. doi:10.11867/j.issn.1001-8166.2019.09.0950

Zhang, H., Zhang, X., and Wen, Z. (2010). *Magnetic anomaly map of geological and geophysical map series of Eastern China and adjacent regions(1:100 0000)*. Beijing: China ocean press.

Zheng, Q., Zhou, Z., Cai, L., Lu, Y., and Cao, Q. (2005). Meso-cenozoic tectonic setting and evolution of east China Sea shelf basin. *Oil &Gas Geol.* 26 (2), 197–201. doi:10.11743/ogg20050210

Zhong, K., Zhu, W., Gao, S., and Fu, X. (2018). Key geological questions of the formation and evolution and hydrocarbon accumulation of the east China Sea shelf basin. *Earth Sci.* 43 (10), 3485–3497. doi:10.3799/dqkx.2018.282

Zhou, D., Chen, H., Sun, Z., and Xu, H. (2005). Three mesozoic sea basins in eastern and southern south China Sea and their relation to tethys and paleo-pacific domains. *J. Trop. Oceanogr.* 24 (2), 16–25. doi:10.3969/j.issn.1009-5470.2005.02.003

Zhou, D. (2002). Mesozoic strata and sedimentary environment in SW Taiwan basin of NE South China Sea and peikang high of Western Taiwan. *J. Trop. Oceanogr.* 21 (2), 50–57. doi:10.3969/j.issn.1009-5470.2002.02.006

Zhou, D., Wang, W., Wang, J., Pang, X., Cai, D., and Sun, Z. (2006). Mesozoic subduction-accretion zone in northeastern south China sea inferred from geophysical interpretations. *Sci. China (Series D)* 36 (3), 471–482. doi:10.1007/s11430-006-0471-9